11th International Conference on Ground Penetrating Radar, June 19-22, 2006, Columbus Ohio, USA

Let the FCC rules work for you: Turning commercial noise into useful data

Evert Slob, Deyan Draganov and Kees Wapenaar
Department of Geotechnology, Delft University of Technology
Mijnbouwstraat 120, 2628 RX, Delft, The Netherlands
e.c.slob@tudelft.nl

***Abstract*— The use of commercial frequency bands for GPR applications with active transmitters becomes more difficult with recent FCC rules in the USA and similar rules in other countries. Especially in the frequency bands where successful shielding of the antennas is very difficult to achieve, other means of acquiring GPR data must be found. The most direct method one can think of is to just record GPR data without using active controlled transmitters, hence, GPR without a source. In this paper we show an example how this can be achieved. Creating new responses from crosscorrelations of responses measured at different locations is known as interferometry. Each newly created response is built from crosscorrelating responses at two receiver locations and represents the field measured at one of the receiver locations as if there were a source in the other receiver location. Recent advances in interferometry suggest that problems that have arisen by the FCC rules may be circumvented by using the principle of interferometry on electromagnetic waves for GPR applications. Here we explore the possibilities and show how noise recordings can be turned into useful signal.**

***Index Terms*— interferometry, noise recordings, crosscorrelation, passive GPR.**

I. INTRODUCTION

Creating new responses from crosscorrelations of responses measured at different locations is known as interferometry. Each newly created response is built from crosscorrelating responses at two receiver locations and represents the field measured at one of the receiver locations as if there were a source in the other receiver location. The first notion of this principle dates back to 1968 [1] when Claerbout showed that for a one-dimensional configuration the acoustic reflection response at the free surface can be created from autocorrelating a transmission response measured at the free surface. This principle was later extended to an arbitrary heterogeneous anisotropic acoustic or elastic medium in a three-dimensional configuration [2], [3], [4].

For open configurations, without a free surface, this extension is equivalent to the configuration where the two receiver locations are inside the domain enclosed by the boundary containing the sources [5]. For exploration geophysics the Earth is probed, hence we restrict ourselves to electromagnetic open configurations. The sources must then lie on a closed boundary. Since usually interferometric techniques rely on conservation of total wave energy, crosscorrelation type techniques cannot be used for recordings of wave phenomena where a substantial part of the wave energy is converted into heat. We show that if the energy loss factor is not high the kinematics of the Green's function are recovered correctly. When the loss factor increases near the boundary sources some artifacts can occur in the form of spurious time-symmetric events, although the kinematics of all desired arrivals are correct. For these simplified representations, we show how they can be used for mutually uncorrelated noise sources. We discuss the effects due to the simplifying assumptions and illustrate them numerical examples at the end of the paper.

II. THEORY

In our paper we use the subscript notation for vectors and tensors, Einstein's summation convention applies to repeated lower case Latin subscripts to which the values 1, 2 and 3 are to be assigned. We use the electric field vector $\hat{\boldsymbol{E}}(\boldsymbol{x},\omega)$, the magnetic field vector $\hat{\boldsymbol{H}}(\boldsymbol{x},\omega)$, and the external source volume densities of electric and magnetic currents, $\{\hat{\boldsymbol{J}}^e(\boldsymbol{x},\omega), \hat{\boldsymbol{J}}^m(\boldsymbol{x},\omega)\}$, respectively. The medium parameters are electric permittivity $\varepsilon_{kr}(\boldsymbol{x})$, electric conductivity $\hat{\sigma}^e_{kr}(\boldsymbol{x},\omega)$, magnetic permeability $\mu_{jp}(\boldsymbol{x})$ and the magnetic conductivity $\hat{\sigma}^m_{jp}(\boldsymbol{x},\omega)$. Note that we have defined the electric permittivity and the magnetic permeability as functions of position only. This is no restriction because the time dependence of these medium parameters can be incorporated in the electric and magnetic conductivities, respectively.

We first show that electromagnetic correlation type interferometric representations can be derived from the electromagnetic reciprocity theorem of the time-correlation type. A reciprocity theorem evaluates two different states, A and B, that can occur in different media and in different domains. For our purposes we apply the theorem to one and the same medium in a single domain, which implies that the medium parameters in the two states are the same. In this situation the frequency domain reciprocity theorem is applied to the domain $\mathbb{D}$ with outward unit normal vector, $\boldsymbol{n}$, is given by

$$\begin{aligned}
&\oint_{\boldsymbol{x}\in\partial\mathbb{D}} n_m\epsilon_{mkj}(\hat{E}^*_{k,A}\hat{H}_{j,B}+\hat{E}_{k,B}\hat{H}^*_{j,A})\mathrm{d}^2\boldsymbol{x}\\
&= -2\int_{\boldsymbol{x}\in\mathbb{D}}[\hat{H}^*_{j,A}\Re\{\hat{\sigma}^m_{jp}\}\hat{H}_{p,B}+\hat{E}^*_{k,A}\Re\{\hat{\sigma}^e_{kr}\}\hat{E}_{r,B}]\mathrm{d}^3\boldsymbol{x}\\
&\quad -\int_{\boldsymbol{x}\in\mathbb{D}}\Big[(\hat{J}^e_{r,A})^*\hat{E}_{r,B}+\hat{J}^e_{k,B}\hat{E}^*_{k,A}\\
&\qquad +\hat{J}^m_{j,B}\hat{H}^*_{j,A}+(\hat{J}^m_{p,A})^*\hat{H}_{p,B}\Big]\mathrm{d}^3\boldsymbol{x},
\end{aligned} \tag{1}$$

where $\Re$ denotes the real part, $*$ denotes complex conjugation and ϵ_{kmj} is the anti-symmetric tensor of rank three, $\epsilon_{kmj} = 1$ when $kmj = \{123, 231, 312\}$, $\epsilon_{kmj} = -1$ when $kmj = \{132, 213, 321\}$, while $\epsilon_{kmj} = 0$ otherwise. For a more detailed treatment of reciprocity theorems and their properties see [6]. The important observations for our purposes are that in equation (1) material parameters that are related to wave propagation do not occur, while the parts of the medium parameters that are related to irreversibly converting energy into heat are present. The latter parts are the real parts of the electric and magnetic conductivities. In absence of conductivities or relaxation mechanisms the first integral on the right-hand side of equation (1) vanishes and we are left with a representation that is indepedent of medium properties. Hence, in principle we can derive results from this representation that are valid for instantaneously reacting, arbitrarily heterogeneous and anisotropic media. For our goal to arrive at representations that can be used in practise we make several assumptions, which are discussed below.

Normally we use electric field receivers and sources and hence in equation (1) we take zero magnetic current sources and write the magnetic field vector in terms of the electric field vector in equation (1). Further we assume a medium with constant scalar magnetic permeability in the neighborhood of the boundary, $\partial\mathbb{D}$, of the domain, $\mathbb{D}$. Substituting all these choices in equation (1) leads to

$$\frac{1}{\mathrm{j}\omega\mu}\oint_{\boldsymbol{x}\in\partial\mathbb{D}} n_m\epsilon_{mkj}\left(\hat{E}^*_{k,A}(\epsilon_{jnr}\partial_n\hat{E}_{r,B}) - \hat{E}_{k,B}(\epsilon_{jnr}\partial_n\hat{E}^*_{r,A})\right)\mathrm{d}^2\boldsymbol{x} = \int_{\boldsymbol{x}\in\mathbb{D}}\left[(\hat{J}^e_{r,A})^*\hat{E}_{r,B} + \hat{J}^e_{k,B}\hat{E}^*_{k,A}\right]\mathrm{d}^3\boldsymbol{x}. \tag{2}$$

The electric current source terms in the right-hand side of equation (2) are used to localize the receivers at $\boldsymbol{x}_A$ and $\boldsymbol{x}_B$. By assuming now also isotropy and homogeneity for the electric permittivity in the neighborhood of the closed boundary surface, $\partial\mathbb{D}$, it can be shown that the left-hand side can be rewritten in terms of time correlations of the electric field and normal derivatives of the electric field. This results in

$$\frac{1}{\mathrm{j}\omega\mu}\oint_{\boldsymbol{x}\in\partial\mathbb{D}}\left(\hat{E}^*_{k,A}n_m\partial_m\hat{E}_{k,B} - \hat{E}_{r,B}n_m\partial_m\hat{E}^*_{r,A}\right)\mathrm{d}^2\boldsymbol{x} = \int_{\boldsymbol{x}\in\mathbb{D}}\left[(\hat{J}^e_{r,A})^*\hat{E}_{r,B} + \hat{J}^e_{k,B}\hat{E}^*_{k,A}\right]\mathrm{d}^3\boldsymbol{x}. \tag{3}$$

We define the observation points in this configuration in terms of the source locations in the two states as $\hat{J}_{k,A} = \hat{s}(\omega)\delta_{kr}\delta(\boldsymbol{x}-\boldsymbol{x}_A)$ and $\hat{J}_{r,B} = \hat{s}(\omega)\delta_{rs}\delta(\boldsymbol{x}-\boldsymbol{x}_B)$. We then define the fields as,

$$\hat{J}_{k,A} = \hat{s}(\omega)\delta_{kr}\delta(\boldsymbol{x}-\boldsymbol{x}_A);\, \hat{E}_{k,A} = \hat{G}_{kr}(\boldsymbol{x},\boldsymbol{x}_A,\omega)\hat{s}(\omega), \tag{4}$$

$$\hat{J}_{r,B} = \hat{s}(\omega)\delta_{rs}\delta(\boldsymbol{x}-\boldsymbol{x}_B);\, \hat{E}_{r,B} = \hat{G}_{rs}(\boldsymbol{x},\boldsymbol{x}_B,\omega)\hat{s}(\omega). \tag{5}$$

Substituing equations (4) and (5) in equation (3) leads to

$$2\Re\{\hat{G}_{kr}(\boldsymbol{x}_A,\boldsymbol{x}_B,\omega)\}|\hat{s}(\omega)|^2 = -\frac{1}{\mathrm{j}\omega\mu} \times\oint_{\boldsymbol{x}\in\partial\mathbb{D}}\Big(\{\hat{G}_{kj}(\boldsymbol{x}_A,\boldsymbol{x},\omega)\hat{s}(\omega)\}^*n_m\partial_m\{\hat{G}_{rj}(\boldsymbol{x}_B,\boldsymbol{x},\omega)\hat{s}(\omega)\} -\{n_m\partial_m\hat{G}_{kp}(\boldsymbol{x}_A,\boldsymbol{x},\omega)\hat{s}(\omega)\}^*\{\hat{G}_{rp}(\boldsymbol{x}_B,\boldsymbol{x},\omega)\hat{s}(\omega)\}\Big)\mathrm{d}^2\boldsymbol{x}, \tag{6}$$

where μ is the magnetic permeability of the medium in the neighborhood of the boundary. This is an exact representation for the electric field Green's function for an electric current source in terms of crosscorrelations of observed wavefields at $\boldsymbol{x}_A$ and $\boldsymbol{x}_B$ inside the domain $\mathbb{D}$. This is true for any heterogeneous anisotropic medium that is homogeneous and isotropic only in the neighborhood of the boundary $\partial\mathbb{D}$. The two terms under the integral of equation (6) ensure that waves propagating outward from the sources at $\boldsymbol{x}$ on $\partial\mathbb{D}$ do not interact with those propagating inward and vice versa. We extend our assumption of a homogeneous and isotropic medium to exist also outside the domain $\mathbb{D}$. Waves that leave the domain $\mathbb{D}$ never enter it again, implying that the boundary is convex seen from the inside of $\mathbb{D}$. It can then be shown with stationary phase analysis [7] that the terms under the integral are approximately equal but with opposite sign, hence

$$2\Re\{\hat{G}_{kr}(\boldsymbol{x}_A,\boldsymbol{x}_B,\omega)\}|\hat{s}(\omega)|^2 \approx -\frac{2}{\mathrm{j}\omega\mu}\oint_{\boldsymbol{x}\in\partial\mathbb{D}} \{\hat{G}_{kj}(\boldsymbol{x}_A,\boldsymbol{x},\omega)\hat{s}(\omega)\}^*n_m\partial_m\{\hat{G}_{rj}(\boldsymbol{x}_B,\boldsymbol{x},\omega)\hat{s}(\omega)\}\mathrm{d}^2\boldsymbol{x}, \tag{7}$$

where now μ is the magnetic permeability of the whole embedding. Finally, if we take the boundary $\partial\mathbb{D}$ to be a sphere with large enough radius such that the Fraunhofer far-field conditions apply, we obtain

$$2\Re\{\hat{G}_{kr}(\boldsymbol{x}_A,\boldsymbol{x}_B,\omega)\}|\hat{s}(\omega)|^2 \approx -\frac{2}{\mu c} \times\oint_{\boldsymbol{x}\in\partial\mathbb{D}}\{\hat{G}_{kj}(\boldsymbol{x}_A,\boldsymbol{x},\omega)\hat{s}(\omega)\}^*\{\hat{G}_{rj}(\boldsymbol{x}_B,\boldsymbol{x},\omega)\hat{s}(\omega)\}\mathrm{d}^2\boldsymbol{x}, \tag{8}$$

where $c = (\varepsilon\mu)^{-1/2}$ is the electromagnetic wave velocity in the embedding. Each integrand in the right-hand side of equation (8) is an electric field generated by a spatial point souce of arbitrary direction and located at position $\boldsymbol{x}$ on the boundary and the k-component is recorded at location $\boldsymbol{x}_A$, while the r-component is recorded at location $\boldsymbol{x}_B$. By crosscorrelating these two recordings in the time domain and then summing over all source locations on the boundary yields the k-component electric field Green's function recorded at $\boldsymbol{x}_A$ and generated by the r-component of a spatial point source at location $\boldsymbol{x}_B$. This Green's function is scaled by the power spectrum of the sources, which has been assumed known.

A. Mutually uncorrelated noise sources

For laboratory applications the expressions of equation (8) are useful as independent measurements are achievable, but in natural environments it will be difficult to satisfy the requirement of independent measurements at each source location and for each source direction. Here we show that this requirement is dropped when we have mutually uncorrelated noise sources. We assume noise sources $\hat{N}_j(\boldsymbol{x},\omega)$ that are mutually uncorrelated in the different directions and in position. When at each surface we have a constant power spectrum $\hat{S}$ such that $\langle \hat{N}_j^*(\boldsymbol{x},\omega), \hat{N}_p(\boldsymbol{x}',\omega)\rangle = Y\delta_{jp}\delta(\boldsymbol{x}-\boldsymbol{x}')\hat{S}(\omega)$, where Y is the plane wave admittance $Y = 1/(\mu c)$ for the whole boundary, we find

$$\Re\{\hat{G}_{kr}(\boldsymbol{x}_A,\boldsymbol{x}_B,\omega)\}\hat{S} \approx -\langle\{\hat{E}_k^{\rm obs}(\boldsymbol{x}_A,\omega)\}^*\hat{E}_r^{\rm obs}(\boldsymbol{x}_B,\omega)\rangle, \quad (9)$$

where the observed electric wavefields are given by

$$\hat{E}_k^{\rm obs}(\boldsymbol{x}_A,\omega) = \oint_{\boldsymbol{x}\in\partial\mathbb{D}} \hat{G}_{kj}(\boldsymbol{x}_A,\boldsymbol{x},\omega)\hat{N}_j(\boldsymbol{x},\omega)\mathrm{d}^2\boldsymbol{x}, \quad (10)$$

$$\hat{E}_r^{\rm obs}(\boldsymbol{x}_B,\omega) = \oint_{\boldsymbol{x}\in\partial\mathbb{D}} \hat{G}_{rp}(\boldsymbol{x}_A,\boldsymbol{x}',\omega)\hat{N}_p(\boldsymbol{x}',\omega)\mathrm{d}^2\boldsymbol{x}'. \quad (11)$$

The spatial average in equation (9) is taken over several realizations of the source distributions, indicated by $\langle\cdot\rangle$ in the right-hand side of equation (9). The time domain equivalent is given by

$$\int_{t'=-\infty}^{\infty}\{G_{kr}(\boldsymbol{x}_A,\boldsymbol{x}_B,-t') + G_{kr}(\boldsymbol{x}_A,\boldsymbol{x}_B,t')\}S(t-t')\mathrm{d}t'$$
$$\approx -2\left\langle \int_{t'=-\infty}^{\infty} E_k^{\rm obs}(\boldsymbol{x}_A,t+t')E_r^{\rm obs}(\boldsymbol{x}_B,t')\mathrm{d}t'\right\rangle, \quad (12)$$

for $\boldsymbol{x}_A \in \mathbb{D}, \boldsymbol{x}_B \in \mathbb{D}$, and expresses that the crosscorrelation of electric field measurements at two locations yields the electric field Green's function and its time-reversed counterpart between those two locations convolved with the autocorrelation of the noise sources. The result in equation (12) is the electromagnetic equivalent of the elastic result in [4]. The advantage is that all sources act simultaneously, avoiding the need for separate measurements.

III. NUMERICAL RESULTS

For equation (12) to be of any use we must be able to identify possible sources to generate the noise fields. Possible noise sources are all human activities and solar activity at GPR frequencies. All these sources are in the air above the surface and that would allow us to use only part of the closed boundary. We will therefore also investigate the effect of having sources distributed only on one side of the domain to be probed. Here we work out a two-dimensional example for GPR.

In the usual GPR acquisition configuration we use two parallel broad-side antennas which reduce to a TE-mode acquisition set up in a 2D setting. We assume that there are several TE-mode line sources of electromagnetic fields in the air and below the bottom interface, located on a straight line. In that case only sources in the air and in the homogeneous lower half space contribute [8]. The observation points are located just above the surface as a model for acquisition with ground coupled antennas. Below the surface a two-layered half plane is considered, each layer being homogeneous. The examples we show come from this three layered model with lateral heterogeneities, upper half space is air and modeled as

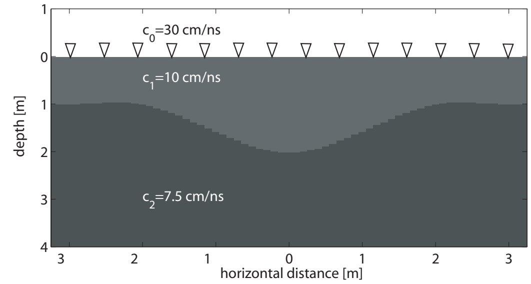

Fig. 1. The model used for the example with noise sources. It has a now there is a syncline in the first layer.

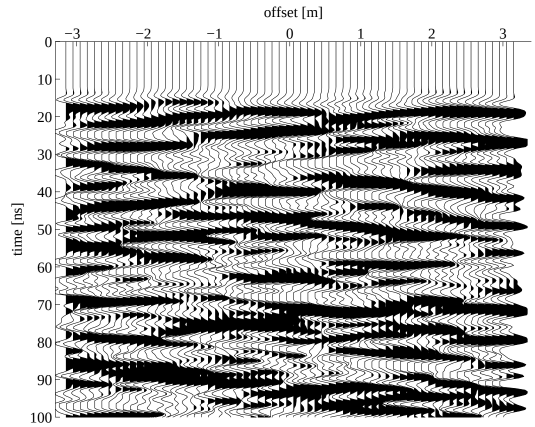

Fig. 2. The first 100 ns of a noise recording from sources in the upper half space only, with 10 cm distance between the recorders. A two-sided CMP, with $x = 0$ as midpoint, can be constructed by autocorrelating the midpoint trace and subsequent crosscorrelating a recording at negative distance with one at the same positive distance.

free space, the second layer has a varying thickness from 1 m to 2 m and the relative electric permittivity is $\varepsilon_r = 9$, while the relative electric permittivity of the lower half space below the syncline is $\varepsilon_r = 16$, see Figure 1. The upper source level, $x_{3;1}$ is 2 m above the surface where the antennas are placed, while the lower source level, $x_{3;2}$, is 1 m below the lowest depth level of the syncline boundary in the lower half space. The sources are separated by 10 cm in the horizontal direction and we have used 128 sources spanning a horizontal offset of 6.4 m in both directions. All sources act at the same time and are mutually uncorrelated. The source time signature of all boundary sources is a random noise signature band limited to two octaves around a 250 MHz center frequency. The earth response to these signals is recorded by 64 receivers located on the surface in the upper half space, also evenly spaced at 10 cm, and which are used to construct a CMP gather. The data from the noise recording are shown in Figure 2 where the first 100 ns of the recording is shown. To construct the CMP from these noise recordings we have used a record length of 120 μs. To compare our results we show first a CMP computed by direct modeling using a Finite Difference code, see Figure 3. The CMP is made with the midpoint directly over the lowest point of the syncline to simulate a CMP over a laterally heterogeneous medium. The five labeled events in Figure 3 are the direct air wave (1), the reflection from the side of the syncline which at larger offsets goes over into a refracted

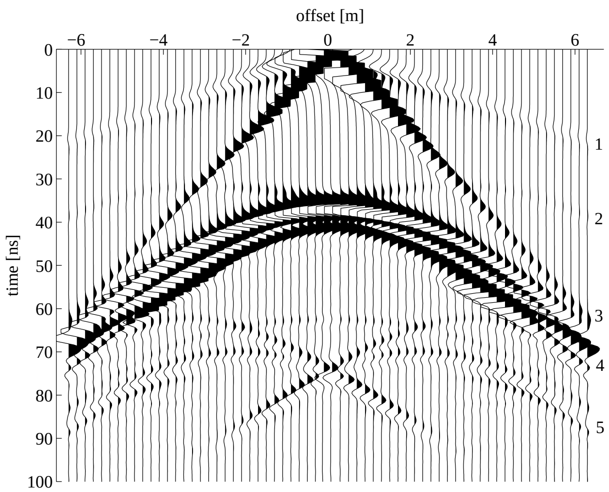

Fig. 3. A two-sided CMP directly modeled with the midpoint directly over the syncline, with 20 cm stepsize.

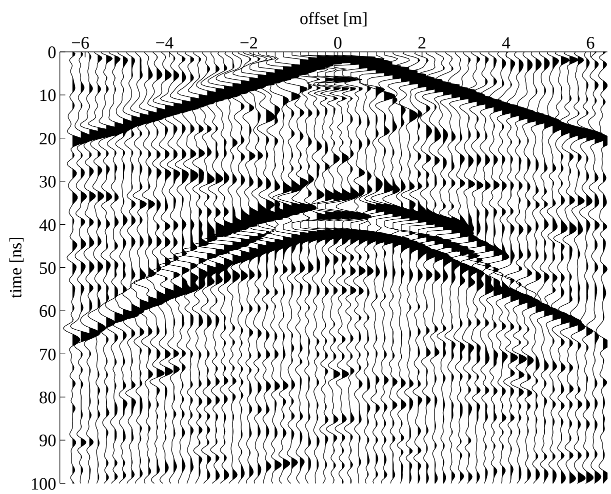

Fig. 4. A two-sided CMP constructed using only noise sources in the upper half space with the midpoint directly over the syncline, with 20 cm stepsize.

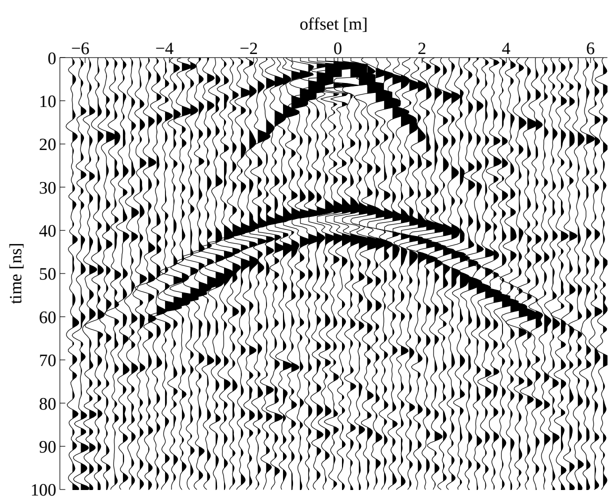

Fig. 5. A two-sided CMP constructed using noise sources in the upper and lower half spaces with the midpoint directly over the syncline, with 20 cm stepsize.

wave in the air (2), the direct ground wave (3), a complicated conglomerate of reflections from inside the syncline (4) and reflections including multiple scattering inside the syncline (5). The most realistic scenario is when we consider only noise sources in the air, while sources in the subsurface are far less likely to be present at GPR frequencies. Therefore, in Figure 4 the result is shown from crosscorrelations using only sources in the top boundary, i.e., in the air above the surface. We observe that the CMP contains all important events, (1), (2) and (4), while the direct ground wave and the multiple scattering effects are almost invisible as they are at the noise level. Some of the complexity of event (4) is recovered but not completely and certainly not with the correct amplitude. The absence of the direct ground wave is understandable from the fact that grazing incidence plane waves that are incident from the air on the earth surface are transmitted into the subsurface at the critical angle. Including the contributions from the bottom boundary sources, increases the amplitude of the direct ground wave, while the accuracy of event (4) has greatly improved within the offset range from -3m to 3m as can be seen in Figure 5. This is understandable from the limited size of the boundary containing the noise sources. Events (2) and (5) are clearly at the noise level and almost invisible.

IV. CONCLUSIONS

From the electromagnetic reciprocity theorem of the time-correlation type an exact interferometric Green's function representation was derived for media that are instantaneously reacting, arbitrarily heterogeneous and anisotropic inside and outside a bounded domain with a closed boundary, where sources of electromagnetic field are present. Under certain conditions, approximations are possible that lead to practical representations. Numerical results suggest that the availability of noise sources in the air above the recording antennas are sufficient to obtain reasonable radargrams.

ACKNOWLEDGMENTS

This work is part of the research program of the Netherlands research center for Integrated Solid Earth Science (ISES). The research of DD is supported by the Dutch Technology Foundation STW under project number DET4915.

REFERENCES

[1] Claerbout, J., Synthesis of a layered medium from its acoustic transmission response, *Geophysics*, *33*, 264–269 (1968).

[2] Wapenaar, C., D. Draganov, J. Thorbecke, and J. Fokkema, Theory of acoustic daylight imaging revisited, *Expanded Abstracts*, 72nd Annual Internat. Mtg. Soc. Expl. Geophys., 2269–2272 (2002).

[3] Derode, A., E. Larose, M. Tanter, J. de Rosny, A. Tourin, M. Campilo, and M. Fink, Recovering the Green's function from field-field correlations in an open scattering medium(L), *JASA*, *113*, no. 6, 2973–2976, doi:10.1121/1.1570436 (2003).

[4] Wapenaar, C., Retrieving the elastodynamic Green's function of an arbitrary inhomogeneous medium by cross correlation, *Phys. Rev. Lett.*, *93*, 254,301–1–4, doi:10.1103/PhysRevLett.93.254301 (2004).

[5] Wapenaar, C., and J. Fokkema, Green's function representations for seismic interferometry, *Geophysics*, *71*, accepted for publication (2006).

[6] de Hoop, A., *Handbook of radiation and scattering of waves*, Academic Press, Amsterdam (1995).

[7] Snieder, R., Extracting the Green's function from the correlation of coda waves: A derivation based on stationary phase, *Phys. Rev. E*, *69*, 046,610–1–8, doi:10.1103/PhysRevE.69.046610 (2004).

[8] Wapenaar, C., G. Geels, V. Budejicky, and A. Berkhout, Inverse extrapolation of primary seismic waves, *Geophysics*, *54*, 853–863 (1989).